MANSOURA JOURNAL OF CHEMISTRY
Official Journal of Faculty of Science, Mansoura University, Egypt
E-mail: scimag@mans.edu.eg ISSN: 2974-4938

Synthesis, spectral characterization, DFT and antioxidant and antihomolysis activities of diamagnetic complexes derived from a new hydrazone derivative

*H. M. El-Sayed, E. Abd-elattif khalifa and O. A. El-Gammal[a]**

Faculty of Science, Chemistry Department, Mansoura University, Mansoura, P.O.Box 70, Mansoura- Egypt

Received:21/8/2022
Accepted: 3/9/2022

Abstract: Novel series of Zn^{2+}, $Cd^{2+}$and Hg^{2+} complexes derived from (E)-2-((3-cyano-4,6-dimethylpyridin-2-yl)thio)-N'-(thiophen-2-ylmethylene)acetohydrazide (HDMAH) in1:1 or 2:1 (L:M) ratio. The complexes were characterized by conventional techniques adopting the molecular formulae; $[Zn(HDMAH)_2Cl(OH)]$, $[Cd(HDMAH)Cl_2H_2OEtOH]$and$[Hg(HDMAH)Cl(OH)EtOH]3EtOH$, respectively. Electronic and infrared spectral dataconfirmed the coordination of HDMAH as neutral ON bidentate in an octahedral environment around metal ion. The structure of Zn^{+2} was also studied by XRD technique. was completed using the DFT method, which was also utilised to assess other energy properties include electronegativity, HOMO, LUMO, and hardness. As well as using TGA and DrTGA to evaluate thermal stability, Coats-Redfern and Horowitz-Metzger techniques were employed to determine the corresponding thermodynamic parameters of activation. Additionally, each molecule was examined for antioxidant using $ABTS^{+}$ free radical scavenger and antihemolytic activities. The biological assay is extended to test the inhibition activity of breast cancer. The results revealed Zn^{+2} possesses a potent activity among all title compounds

Keywords: novel hydrazones, NMR, neutral ON, and antioxidant activity.

1.Introduction

Hydrazones, in medicinal chemistry are frequently used as potent intermediates in the synthesis of pharmacological and bioactive molecules because of their wide range[1-3]. Additionally, hydrazones have been widely used in the textile sector in addition to the manufacture of plastics, photographic films, and dyes [4-8]. Their compounds with transition metal ions have gained a lot of focus in both industry and biology[9]. Such metal complexes have made it clear that nitrogen and oxygen coordination play a key role in these compounds, which has led to the identification of their many chelation modes[10-15]. The outstanding antibacterial, anticancer [16-17], antiviral [18-19], antimalarial, antioxidant, and antitumor [20-24] actions of these prospective ligands were likely the primary driving force behind establishing the coordination chemistry of them. Therefore, It is evident that creating synthetic pathways to change, replace, or substitute the resultant hydrazone will enable the identification of the molecular characteristics required for such actions. Therefore, This work's objective is to describe. the synthesis and clarify the structure of a new hydrazone. namel(E)2-((3-cyano-4,6dimethylpyridin-2-yl)thio)-N'-(thiophen-2-ylmethylene)acetohydrazide (HDMAH) and its Zn^{2+}, Cd^{2+} and Hg^{2+}. The work includes also the investigation of the antioxidant and anti-hemolytic properties within the title compounds.

2. Experimental

2.1. Chemicals

All the chemicals used in the extraction and fractionation procedures were of analytical grade, obtained from Sigma-Aldrich (St. Louis, MO, USA), and used as received. HPLC-grade solvent was used for the GC-MS analysis.

2.2. Equipment

Electronic spectra were displayed using Perkin-Elmer UV-visible spectra using the AA800 spectrophotometer Model AAS with a 1.0 cm cell model. IR spectra were captured

using a Jasco FTIR-4100 spectrophotometer (KBr discs, 4000-400 cm^{-1}), 1H NMR and 13C NMR spectra were shown using Bruker WP operating at 300 and 80 MHz, respectively, Perkin Elmer ChemBio3D software was used to create the chemicals specifically [25].Using a nitrogen atmospheric Shimadzu thermogravimetric analyzer with a heating rate of 15 °C/min throughout a range of temperatures from room temperature to 800 °C, thermal analysis data of the ligand and the complexes were obtained.

2.3. Synthesis of from (E)-2-((3-cyano-4,6-dimethylpyridin-2-yl)thio)-N'-(thiophen-2-ylmethylene)acetohydrazide (HDMAH)

0.234 gm of 2-((3-cyano-4,6-dimethylpyridin-2-yl)thio)acetohydrazide (1mmole) were added to thiophene-2-carbaldehyde (1mmol) in presence of 15ml ETOH. The mixture for the reaction was reflux heated for three hours while being stirred. The resulting pale-yellow precipitate was filtered out, after being completely rinsed with cold water, dried in a sterile desiccator over anhydrous $CaCl_2$. TLC, IR, and 1HNMR were used to test the product. The data of physical properties are listed in Table 1.

2.4. Synthesis of metal complexes

An ethanolic solution of HDMAH (0.330 g, 1 mmol) had been added, and the mixture was heated using a reflux system for 3–4 hours with the matching metal chloride ($MCl_2.2H_2O$; M= Zn^{2+}, Cd^{2+}, and Hg^{2+}; x =2) in hot ethanolic solution. After being filtered out, The precipitates were cleaned with ethanol and then diethyl ether before being dried in a vacuum desiccator over anhydrous $CaCl_2$ and analysed with TLC and elemental analysis (C, H, N, M, and Cl), and spectroscopic tools (IR, UV-Vis.,). There are complexes soluble in non-electrolytes, as well as in air (1–15 ohm^{-1} cm^2 mol^{-1}), dimethylformamide (DMF), and dimethyl sulfoxide (DMSO) [26]. There were numerous unsuccessful attempts to isolate a single crystal. The physical and analytical data are listed in Table 1.

2.5. Biological activity

2.5.1. Antioxidant activity

The assay uses a stable free radical, the radical cation of 2, 2′-azino-bis (3-ethyl Benzthiazoline-6-sulfonic acid) (ABTS) to evaluate antioxidants and extracts.

2.5.1.1. ABTS free radical scavenging activity

The reaction mixture for the negative control consists of 3 ml of MnO2 solution (25 mg/ml) and 2 ml of 2,2′-azino-bis- (3-ethylbenzthiazoline-6-sulfonicacid) solution, both prepared in phosphate buffer (pH=7) [27]. The mixture was stirred, centrifuged, the excess oxide was then filtered out. The resulting green-blue solution's absorbance ($A_{control}$) ($ABTS^+$ radical solution) was recorded at λ_{max}=734 nm. After adding 20 µl of the test sample's 1 mg/ml solution in spectroscopic grade MeOH/buffer (1:1 v/v) to the ABTS solution, the absorbance (A_{test}) was calculated. Ascorbic acid 20 µl (2ml) solution served as a standard antioxidant (positive control). Solvent was used without ABTS to run a blank sample. The decrease in absorbance is expressed as % inhibition.

2.5.1.2. Antioxidant activity screening assay for erythrocyte hemolysis

Rats' hearts were punctured to get the blood, It was then gathered in tubes that had been heparinized. The buffy coat underwent three rounds of washing in 10 litres of 0.15 M NaCl after being separated into plasma and erythrocytes. The erythrocytes were centrifuged for 10 min. at 2500 rev/min. during the final wash to produce a continuously packed cell preparation. During this test technique, peroxyl radicals were the mediators of erythrocyte hemolysis [28]. In order to analyse samples containing various concentrations of 200 mM AAPH solution in PBS, A 10% suspension of erythrocytes in PBS is added (phosphate buffered saline, pH 7.4). The two hours that the reaction mixture was incubated at 37 °C were spent gently shaking it. After being diluted with eight volumes of PBS, the reaction mixture was removed and centrifuged at 1500 g for 10 minutes. At 540 nm, the supernatant's absorbance was measured. Similar to the above, 8 volumes of distilled water were added to the reaction mixture to fully achieve hemolysis. The absorbance of the supernatant produced after centrifugation was then measured at 540 nm. A positive control was utilized, L-ascorbic acid. examination using a hemocytometer and

using trypan blue stain (stains only the dead cells) [28].

2.6. Molecular modeling

The cluster estimations [29] and double numerical basis sets plus polarisation functional (DNP) implemented in Materials Studio bundle [30] were investigated using DMOL3 module computations. It's made to carry out large-scale density functional theory (DFT) calculations [31,32]. The geometric optimization is done without regard for symmetry.

3. Results and discussion

3.1. IR spectra

The IR spectral data of investigated compounds are listed in Table 1 and figure (1a & 1b). The HDMAH Schiff base's IR spectra revealed two bands at 1662 and 1624 cm^{-1} that are attributed to the stretching vibration mode of the (C=O) group [33], This suggests that the Z and E conforms have the ligand.

The $\nu(C=N)_{azomethine}$ vibration bands at 1583 cm^{-1}, which were observable at 1572–1577 cm^{-1}, undergo a blue shift after complexation. Middle intensity band found at 1132 cm^{-1} is associated to the (N-N) mode, whilst the one found at 1597 cm^{-1} is related to the $(C=C)_{thiophene}$. The two bands of the two isomers that appeared to be broadband at 3202 and 3237 cm^{-1} for a shoulder are attributed to the two forms' (NH) vibrations in the solid state. At 689 cm^{-1}, the band caused by ν(C-S)thiophen is visible, but the band at 721 cm^{-1} can be attributed to the (C-S-C) vibrational mode. The bands seen at 1583, 997, 644 and 404 cm^{-1} are assigned to stretching mode$(C=N)_{pyridine}$ overlapped with $\nu(C=N_{)azomethine}$, pyridine- ring breathing modes as well as its (C=N)pyridine out-of-plane ring vibration and in-plane bending modes [34]. The stretching vibrations of symmetric and asymmetric aliphatic CH_3 groups, which are converted to a weak doublet in metal complexes' IR spectra , are responsible for the doublet bands at 2928 and 2963 cm^{-1} [34]. The sharp band seen at 2216 and 834 cm^{-1} may be caused by ν (CN) in the meta position to N of the pyridine ring.

In $[Zn(HDMAH)_2$ Cl (OH)] (Structure 2) and [Cd(HDMAH) Cl_2 H_2O EtOH] (Structure 3) complexes, HDMAH behaves as neutral NO bidentate via O atom of C=O and N of $(C=N)_{azomethine.}$ Weakness and a slight shift of bands ascribed to ν(C=O) and$(C=N)_{azomethine}$to lower wavenumber [35] confirm this supposed mode of chelation. The band that can be assigned to $(C-S)_{thiophen}$ and (NH) stay the same at the same places, showing that they are not taking part in coordination. The (OH) mode in both complexes is responsible for the bands at 3312 and 3320 cm^{-1},respectively.

In [Hg(HDMAH)Cl(OH)EtOH]3EtOH, the ligand binds the metal ion in neutral manner as NOS tridentate through O atom of C=O, N of $(C=N)_{azomethine}$ and S of thiophene ring. The bands' shift to a lower wavenumber as a result of these groups reveals this. However, the band at 3540 cm^{-1} in the final complex is caused by coordinated water signals caused by DMSO (2.50; 3.43ppm). The support for this notification will come from thermal analysis.

3.2. NMR spectra

The 1H NMR spectrum of the ligand in d6-DMSO (Fig. 2a), shown in DMSO-d6, reveals the hydrogen signals' replication. assuming that an existing potential (E/Z) isomerism of the imine double bond is the cause of these duplications. Four singlet signals were visible in the spectrum at H 11.66, 11.58, and 11.43 ppm, corresponding to two NH groups and one OH (enol form). Since each signal represented one proton, this may mean that four theoretical conformations (E), (Z), keto, and enol were present (Fig.1).This is confirmed by the Infrared range of the ligand that should bands assigned to C=O (1662, 1642; 3414, 3202 (NH) in addition to band at 3449 cm^{-1}.The presence of signals due to two methyl group protons in the up field area as singlet at δ_H 2.39-2.74 ppm in addition to the singlet signals at δ_H 4.039 and 4.448ppm for the (-CO-CH_2-S-) groups are a further evidence of the suggested isomerism. Two singlets superimposed on each other at H 8.41 and 8.23 ppm for two protons and a singlet at H 8.20 ppm for the proton of the CH of the pyridine ring were the indications of azomethine protons [35]. The signals of 2-thiophenyl groups, on the other hand, were discovered at H 7.43 (d, J = 5Hz, 4H-5), 7.42 (d, J = 5Hz, 4H-5), 7.127 (d, J = 3.5Hz, 4H-3), 7.124 (d, J = 3.5Hz, 2H-3), 7.11 (d, J = 3.5Hz, 2H-3), 7.12 (m, 4H-4) and 7.08 (m, 4H-4).There were signals due to aliphatic protons

of two CH_3 associated with the pyridine ring at δ =2.37, 2.49 ppm (s, $2CH_3$ group) and the other Also, At H 7.64 (d, J = 5Hz, 4H-5), 7.56 (d, J = 5Hz, 4H-5), 7.43 (d, J = 3.5Hz, 4H-3), 7.39 (d, J = 3.5Hz, 2H-3), 7.37 (d, J = 3.5Hz, 2H-3), 7.12 (m, 4H-4) and 7.01 (m, 4H-4) the signals of 2-thiophenyl groups were discovered [35].

3.3. Electronic spectra and magnetic moments

The electronic spectrum of HDMAH displayed in DMSO is represented in fig.3 that exhibited two shows two broad bands at 45662 cm^{-1} (219.00nm); 29850 cm^{-1} (335.01nm) & 25839 (387 nm), presumably arising from π→π* and n→π*, a combination of the transitions due to those of heterocyclic rings, carbonyl and azomethine groups, respectively [35]

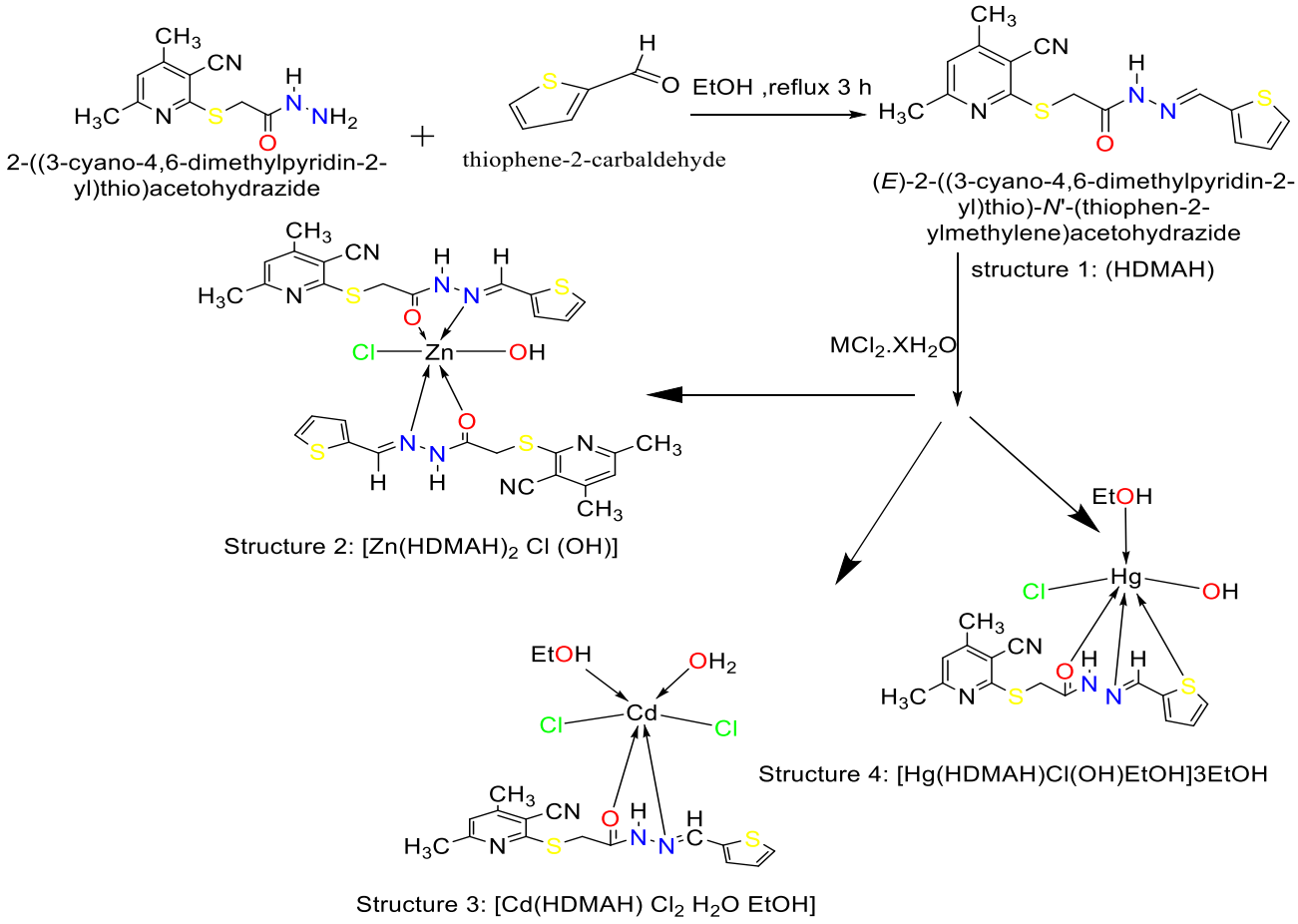

Scheme1: Preparation of HDMAH and its metal complexes

Table (1): Analytical and physical data of HDMAH and divalent metal complexes.*: obtained by mass spectra

Compound	F.wt.Found (Calcd)	Color	M.p.◦c	Elemental analyses% Found (Calcd)				
				C	H	N	Cl	M
HDMAH$C_{15}H_{14}N_4OS_2$	330.00*(330.42)	Paleyellow	225	55.03 (54.50)	5.20(4.27)	16.10(16.91)	.	-
[Zn(HDMAH)$_2$ Cl(OH)] $C_{30}H_{29}N_8O_3S_4ZnCl$	778.68*(778.67)	Yellow	260	46.70 (46.20)	4.60(3.71)	14.81(14.30)	4.50 (5.40)	8.30 (8.90)
[Cd(HDMAH) Cl_2 (EtOH) H_2O] $C_{17}H_{22}N_4O_3S_2CdCl_2$	577.85(577.81)	orange	270	36.20 (35.30)	4.30(3.80)	9.83(9.60)	11.51 (12.22)	19.78 (19.40)
[Hg(HDMAH)Cl(OH)Et O]3EtOH$C_{23}H_{39}N_4O_6S_2H$ gCl	(767.76)	white	275	36.90 (35.90)	4.50 (5.10)	8.00(7.32)	5.33 (4.68)	26.57 (26.10)

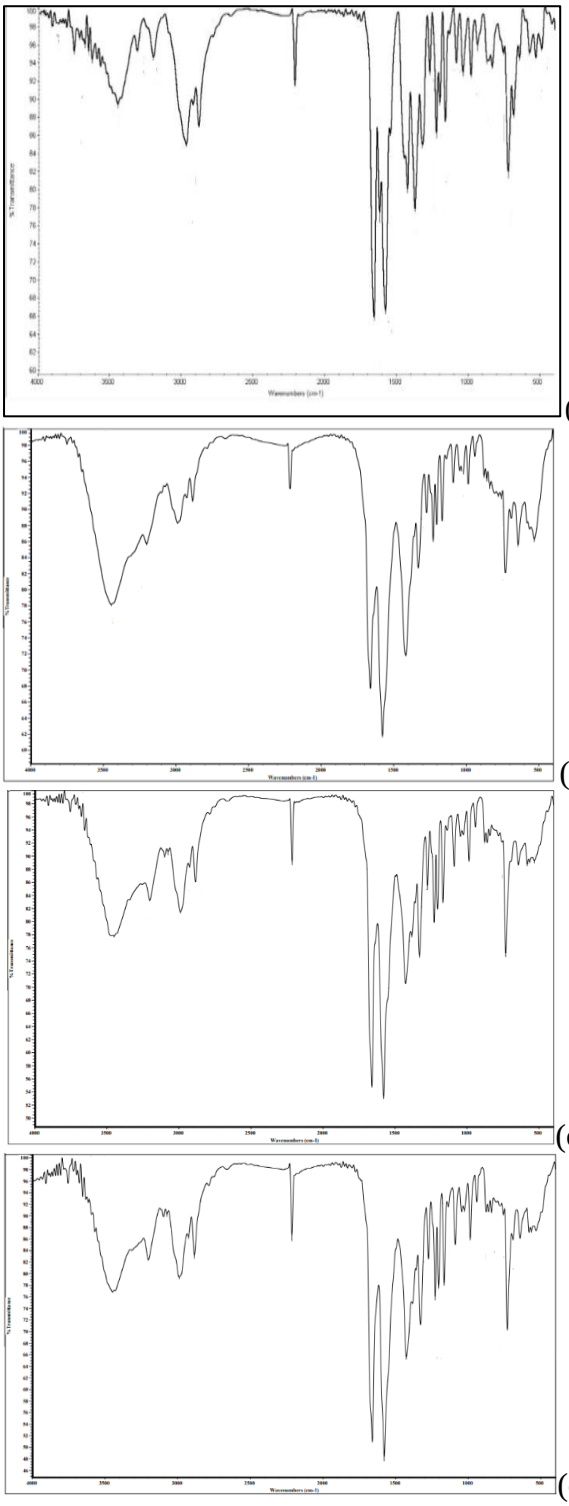

Fig.(1) IR spectral bands of (a) (HDMAH), (b) [Zn(HDMAH)$_2$ Cl (OH)]complex, (c) [Cd(HDMAH) Cl$_2$ (EtOH) H$_2$O] and (d) [Hg(HDMAH)Cl(OH)EtOH]3EtOH.

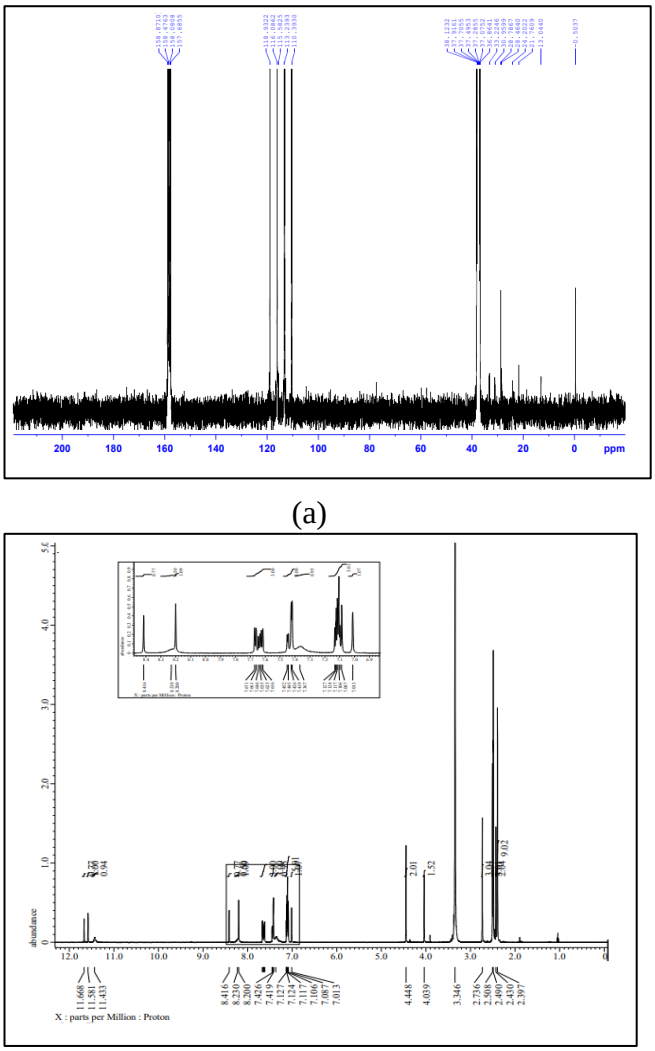

Fig.(2): NMR spectra of HDMAH in d$_6$DEMSO.(a) ^{1}HNMR, (b) ^{13}CNMR

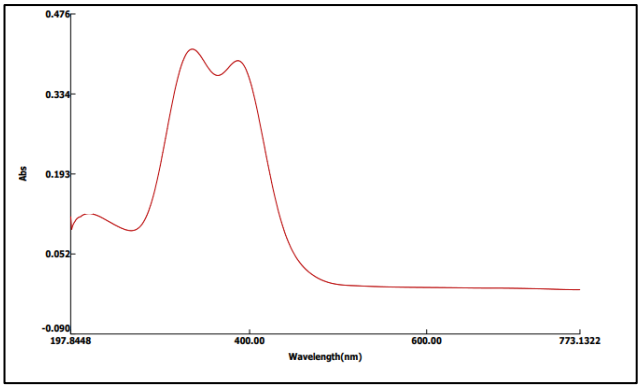

Fig.(3). UV-vis. Spectra in DMSO HDMAH ligand.

Table(2): Assignment IR bands of HDMAH and its divalent metal complexes

Compound	ν(OH)	ν(NH)	ν(C=O)	ν(C=N)	ν(N-N)	ν(C=N)$_{py}$	ν(C-S)	ν(M-O)	ν(M-N)
HDMAH	3314	3202	1662	1548	1043	1583	727	-	-
[Zn(HDMAH)$_2$ Cl (OH)]	3445	3312	1660	1416	1045	1577	838	642	531
[Cd(HDMAH) Cl$_2$ (EtOH) H$_2$O]	3450	3202	1660	1428	1089	1578	859	643	532
[Hg(HDMAH)Cl(OH)EtOH]3EtOH	3448	3201	1659	1426	1045	1577	839	643	533

3.4. Thermal study

Table 3 contains all data, including decomposition stages, temperature range, decomposition product, and weight loss percentages for the current ligand, HDMAH, and its metal complexes, as well as their TGA curves are graphically shown in Figure 4.TG (thermogram) of Zn(II) (fig.4b) as an example, the first decomposition step occurs at (218-311^{o}C) with weight loss (found:24.57%; Calcd. 23.83%) is corresponding to the removal of $2H_2O+HCl+C_5HN+2CH_3+CN$ fragments. The third step (312-413^{0}C) with weight loss (found:20.65%; Calcd. 21.35%) is due to removal of $2C_4H_3S$ fragments after which the thermal decomposition stops and a residue comprising the chelate rig in addition to the organic fragment; ($ZnO+2CH_3+CN+C_5HNS+C_2H_2+HN_2$).

3.5. Thermodynamic and kinetic studies

Coats-Redfern [36] and Horowitz-Metzger [37] methods were used to estimate kinetic parameters of studied compounds and the data are represented graphically in fig. 5 and 6 and table 4. It is obvious that ΔS*(entropy of activation),which is negative, demonstrates that active fragments are more organized than un-decomposed ones. the values ΔH* (enthalpy of activation) are positive indicating an decomposition processes are endothermic. Due to the covalent nature of their bonds, the high values of E_a indicate that such chelates are highly stable. The fact that all breakdown stages are nonspontaneous and growing regularly is also indicated by the positive sign of G*, which is related to the rigidity of the residual complex's structure after one or more ligands have been expulsed [38].

3.6.DFT Study

DFT method is one that conveys the chemical reactivity as well as the site selectivity of molecular systems. The energies of the frontier molecular orbitals (E_{HOMO}, E_{LUMO}) (figs.7-10 C & D) and table 5, the energy band gap which explains the eventual charge transfer interaction within the molecule, electronegativity (v), chemical potential (l), global hardness (g), global softness (S) and index of global electrophilicity (x) [39] are evaluated according to literature [39] and the data recorded in Table 6. This new reactivity index calculates the energy stabilization that occurs when the system picks up extra environmental electronic charge. In determining the reactivity and stability of molecules, g and r are crucial. The ideas of the chemical potential l and the parameters v are connected. We can conclude the following from the data that absolute hardness g and absolute softness r are essential properties to assess the stability and reactivity of molecules. Compared to a hard molecule's large energy gap, a soft molecule has a small energy gap. Soft molecules provide more electron donations.

3.6.1. Molecular electrostatic potential (MEP)

One can use the MEP's constant electron density to plot the electrostatic potential on the surface. The study of molecular structures and their relationships to physiochemical properties, as well as interactions involving hydrogen bonds, can both benefit greatly from it [40]. At a given position r (x, y, z), the electrostatic potential V(r) is defined as the interaction energy between the electrical charge produced by the molecule's electrons, nuclei, and proton located at r. With the help of the C-point and several k-points, the electrostatic potential of molecules may be calculated. In the current work, molecule electrostatic potential (MEP) graphs in three dimensions (3D) for the ligands have been produced (Figs. 9–12B). The maximum negative region, which location would be best The greatest positive zone, which is the ideal location for nucleophilic attack, is given in bluer and is depicted in red for electrophilic attack. Red exhibits the strongest repulsion whereas blue exhibits the strongest attraction when the potential increases in the order of red < green <blue. Electronegative atoms are covered by regions with a negative potential, and hydrogen atoms are covered by regions with a positive potential

3.6.2. Geometry optimization

The following significant observations can be drawn from Tables 6 and 7, which give the bond lengths and bond angles, respectively.

i. When coordination binds complex, they elongate, which lowers the energy required for the bond to vibrate and, in turn, lowers the frequency of vibration, which is consistent with IR frequency readings from experiments.

ii. For HDMAH, the bond lengths; N(15)–C(14), C(15)-C(16) and N(12)-N(14) become significantly longer in the complex as coordination occurs through the (C=N) azomethine group. while C(11)–O(13) bond length of C(11)–O(13) is shortened revealing coordination *via* C=O groups and large strength of M-O bond [40

iii. On coordination, the bond angles of the hydrazone moiety are somewhat changed; the largest alterations effect the C(15)–N(14)–N(12), S(20)-C(10)-C(15), O(13)–C(11)–N(12), O(13)–C(11)–C(10), H(32)-N(12)-C(11), N(14)-N(12)-C(11), and H(31)– C(10)-C(11) [41].

3.7. biological assay

3.7.1. ABTS$^+$ free radical scavenging activity

All compounds were tested for antioxidant activity using ABTS$^+$ assay. An inspection to the data (table 8) in indicates that Following HDMAH in terms of antioxidative activity were Zn(II) and Cd(II) complexes. Hg(II) complex, but on the other hand, displayed a modest level of activity [42].

3.7.2.2 Erythrocyte Hemolysis

Table 9 lists the outcomes of the assay to calculate the rate of erythrocyte hemolysis. According to the table, Zn(II) complex demonstrated the highest level of activity among the compounds, on par with the positive control's (4.08%) level. So, in terms of hemolysis, Zn(II) complex produced the best results in reducing the hemolytic effect of hydrogen peroxide. In other words, based on erythrocyte hemolysis, the compounds can be arranged in the sequence: Zn (II) complex >Cd(II) complex > HDMAH > Hg(II) complex [43].

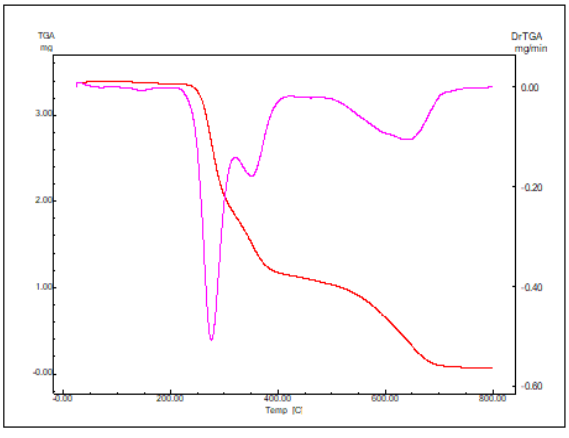

(a)

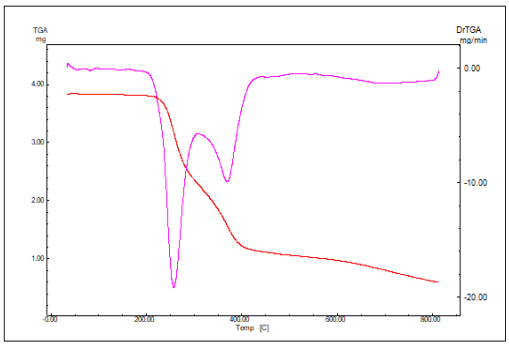

(b)

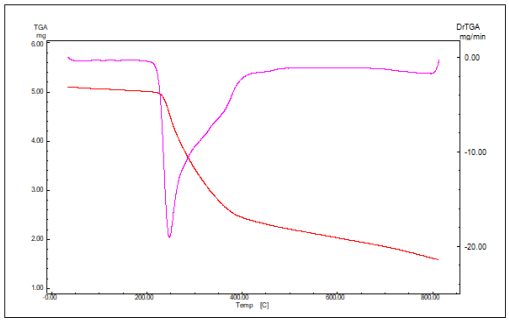

(C)

Fig.(4).TGAcurves.HDMAH(a),[Zn(HDMAH)$_2$ Cl (OH)]complex(b), [Cd(HDMAH) Cl_2 (EtOH) H_2O] complex(c).

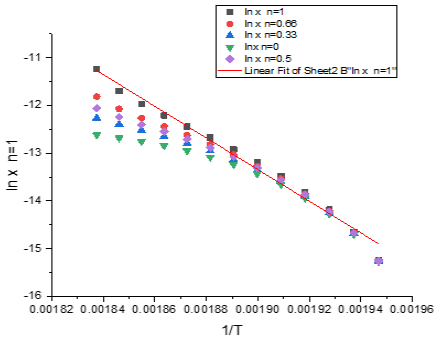

(a)

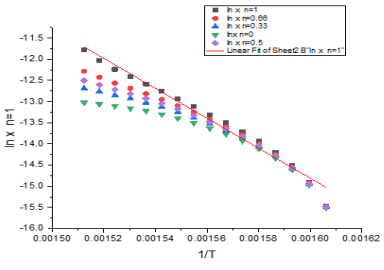

(b)

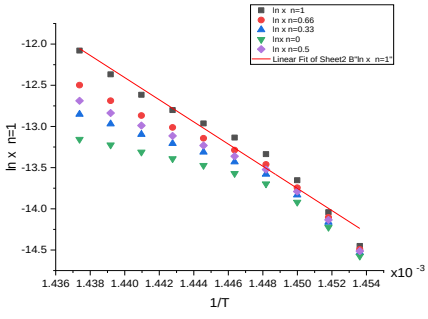

(c)

Fig.(5). Coats-Redfern plots of [Zn(HDMAH)$_2$ Cl (OH)] first degradation step (a), second degradation step (b), third degradation step (c).

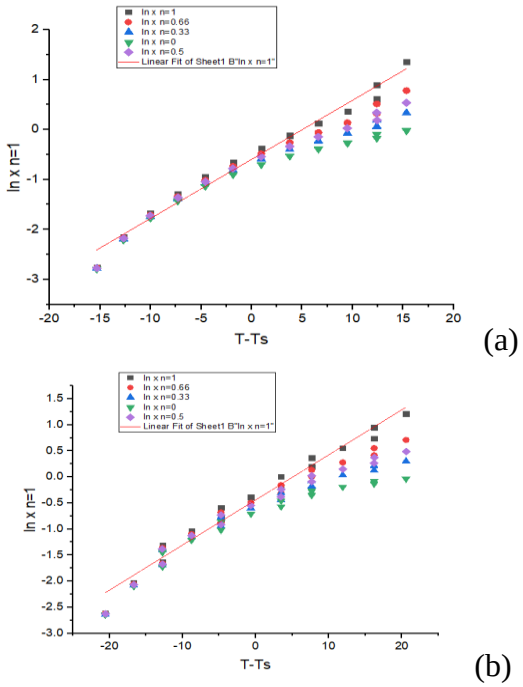

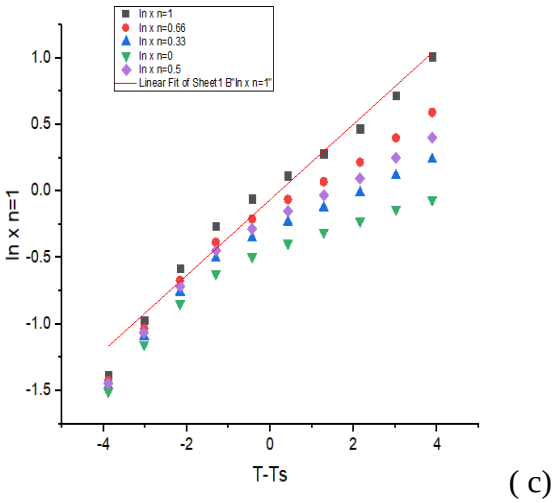

(c)

Fig (6). Horowitz-Metzger plots of $[Zn(HDMAH)_2 Cl (OH)]$. first degradation step (a), second degradation step (b), third degradation step (c).

Table (3): Decomposition steps with the temperature range and weight loss for HDMAH and its divalent metal complexes

Compound	Step	Temp. rang (C)	Removed species	Wt. loss%	
				Found	Calcd
HDMAH	1st	216-304	$-2CH_3+CN+C_5HN$	40.55	39.69
	2nd	305-404	$-C_4H_3S$	24.22	25.15
	3rd	405-711	$-CH_2N_2O+H_2S$	26.30	27.87
	Residue	712-800	2C	7.30	7.27
$[Zn(HDMAH)_2$ Cl (OH)]	1st	218-311	$-2H_2O+HCl+C_5HN+2CH_3+CN$	24.00	23.83
	2nd	312-413	$-C_3HN_2O + H_2S$	15.50	16.32
	3rd	414-469	$-2C_4H_3S$	22.00	21.35
	Residue	470-800	$ZnO+2CH_3+CN+C_5HNS+C_2H_2+HN_2$	37.32	38.22
[Cd(HDMAH) $Cl_2 H_2O$ (EtOH)]	1st	224-280	$-2HCl+H_2O+EtOH$	22.83	23.71
	2nd	281-432	$-C_4H_3S+C_3N_2O+H_2S$	35.22	34.13
	Residue	433-800	$Cd+C_5HN+2CH_3+CN$	41.30	42.14

Table (4). Kinetic parameters evaluated by Coats-Redfern and Horowitz equations for and HDMAH and their divalent (II) complexes.

Compound	peak	Mid Temp(K)	EaKJ\mol	A(S^{-1})	ΔH*KJ\mol	ΔS*KJ\mol.K	ΔG*KJ\mol
HDMAH	1st	546.86	316.97	3.43E+28	312.42	0.2963	150.37
		547.35	325.80	2.41E+29	321.25	0.3125	150.20
	2nd	612.59	171.63	4.84E+12	166.54	-0.0081	171.47
		612.35	182.28	4.08E+13	177.19	0.0097	171.27
	3rd	899.92	218.68	2.90E+10	211.20	-0.0538	259.64
		899.90	235.04	2.69E+11	227.56	-0.0353	259.33
$[Zn(HDMAH)_2$ Cl (OH)]	1st	528.15	275.76	3.11E+25	271.37	0.2384	145.48
		528.15	274.54	2.33E+25	270.15	0.2359	145.53
	2nd	641.68	294.09	4.50E+30	288.75	0.1717	178.58
		641.68	296.22	1.81E+22	290.89	0.1748	178.71
	3rd	692.05	1118.61	1.91E+83	1112.86	1.3424	183.85
		691.825	1129.752	1.34E+84	1124	1.3580	184.11
[Cd(HDMAH) $Cl_2 H_2O$ (EtOH)]	1st	521.06	346.92	1.45E+33	342.59	0.3853	141.83
		521.38	354.96	9.37E+33	350.63	0.4008	141.67
	2nd	587.97	141.03	3.42E+10	136.14	-0.0489	164.89
		587.32	150.62	2.53E+11	145.74	-0.0322	164.67

*Values in Italic: those evaluated by Horowitz.

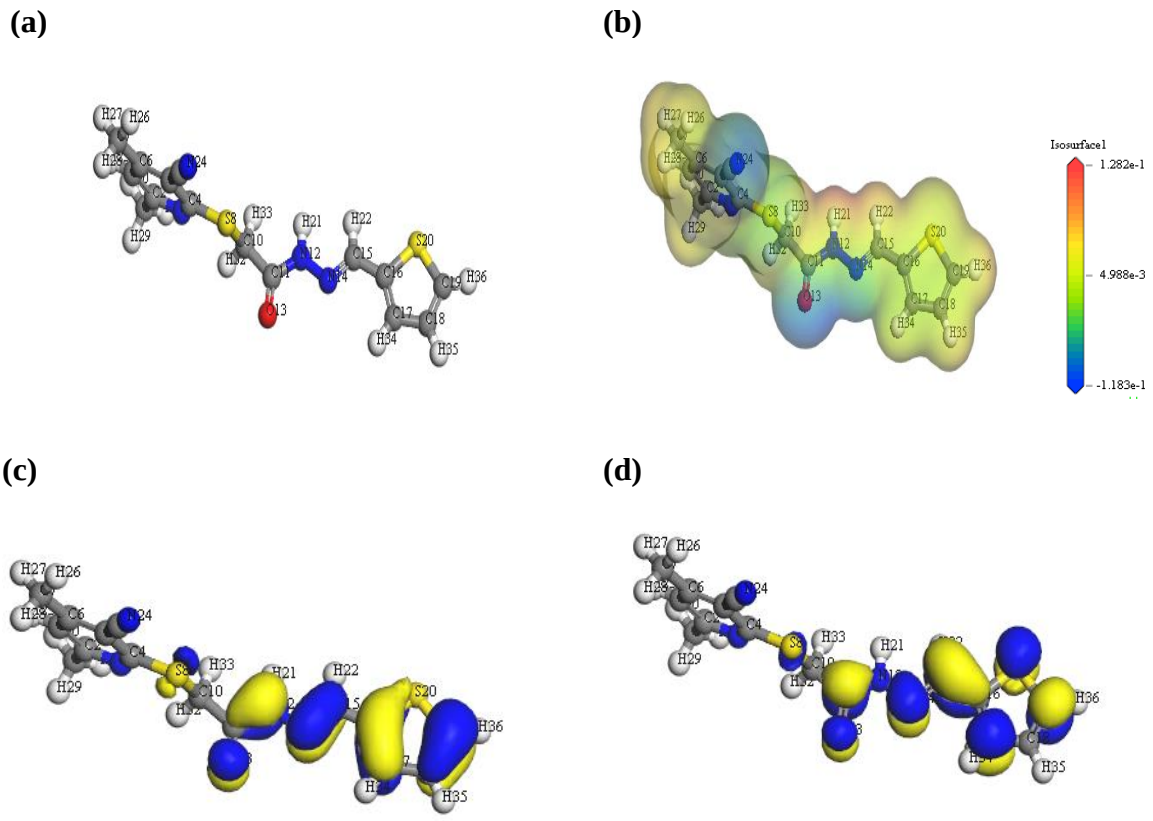

Fig. (7). Molecular modeling of HDMAH. Geometry optimization (a), MEP (b), HOMO(c), LUMO

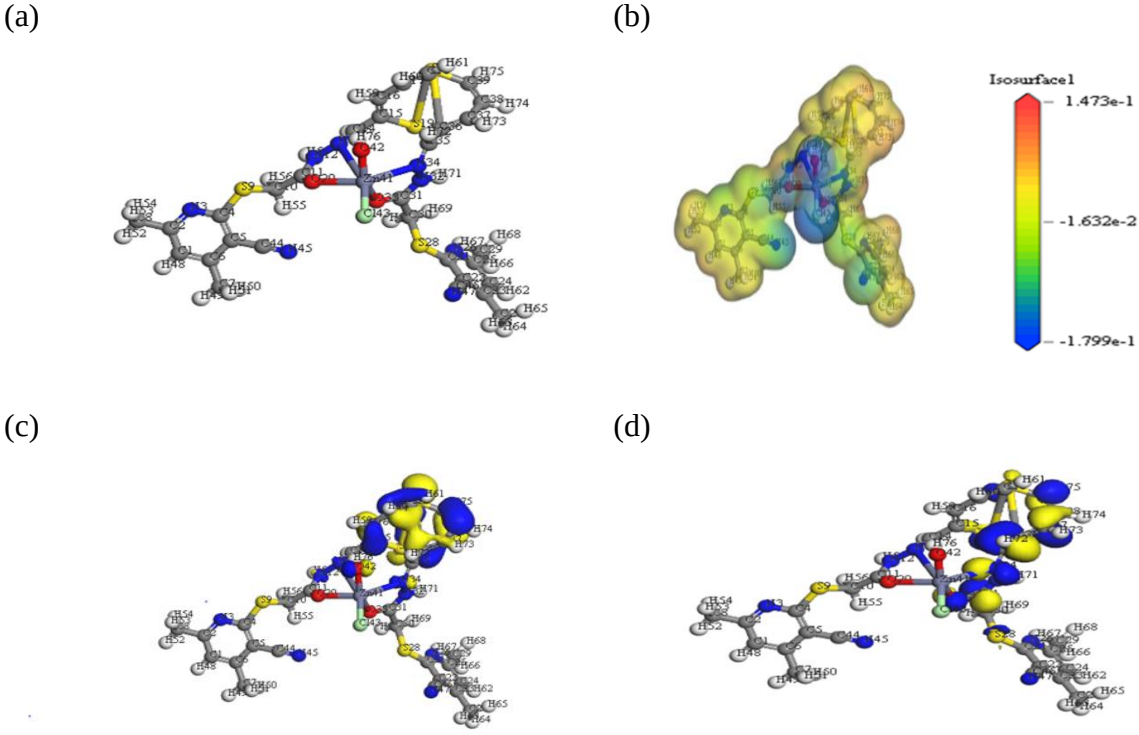

Fig.(8). Molecular modeling of [Zn(HDMAH)$_2$ Cl (OH)]. Geometry optimization (a), MEP (b), HOMO(c), LUMO (d).

(a) (b)

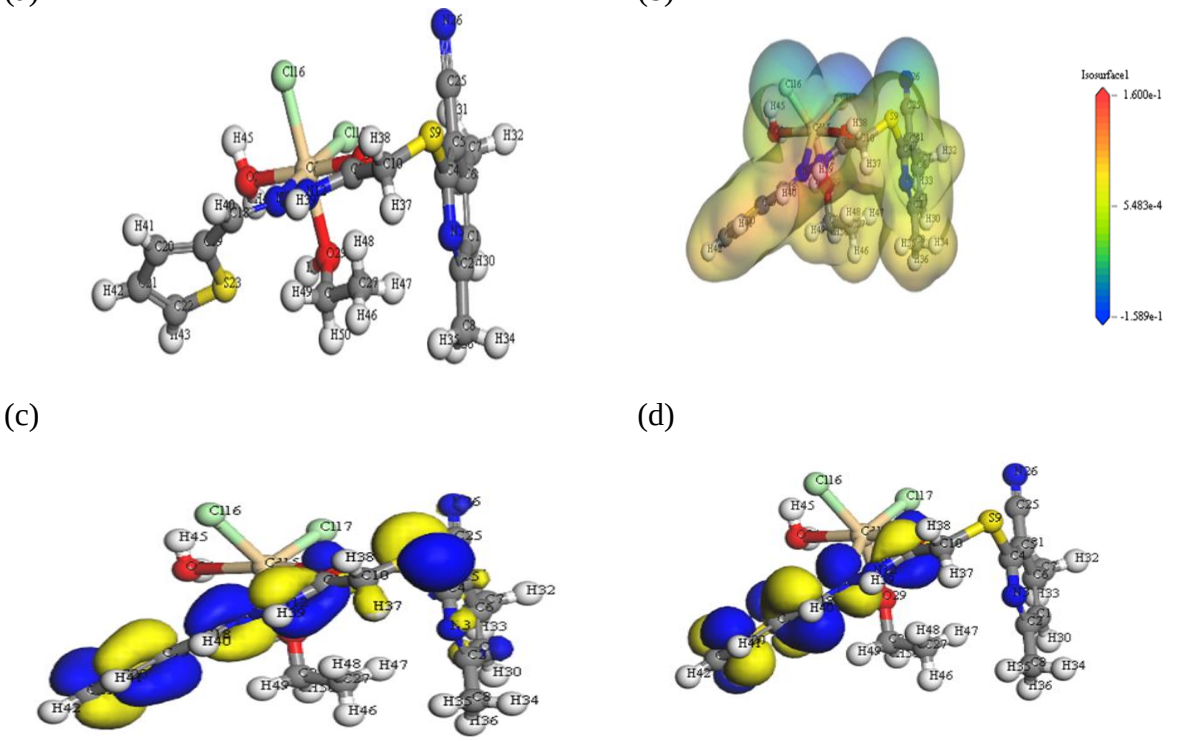

(c) (d)

Fig.(9). Molecular modeling of [Cd(HDMAH) Cl_2 (EtOH) H_2O] Geometry optimization (a), MEP (b), HOMO(c), LUMO (d).

(a) **(b)**

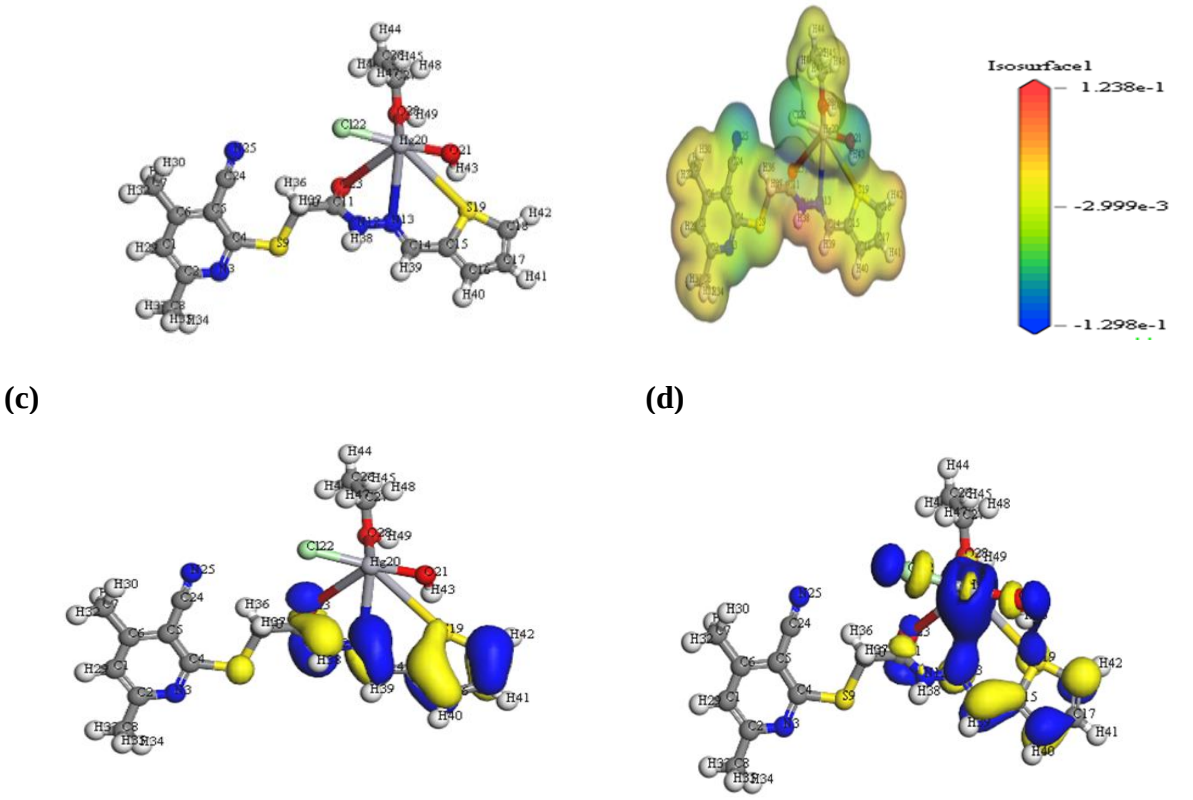

(c) **(d)**

Fig. (10). Molecular modeling of [Hg(HDMAH)Cl(OH)EtOH]3EtOH. Geometry optimization (a), MEP (b), HOMO(c), LUMO (d).

Table (5). Calculated E_{HOMO}, E_{LUMO}, energy band gap ($E_H - E_L$), chemical potential (μ), electronegativity (χ), global hardness (η), global softness (S), global electrophilicity index (ω) and softness (σ) for of HDMAH and its M(II) complexes.

Compound	E_{HOMO}	E_{LUMO}	E_H-E_L	X	μ	η	S	ω	σ
HDMAH	-5.322	2.565	2.757	3.943	3.943	1.378	0.362	5.640	0.725
$[Zn(HDMAH)_2$ Cl (OH)]	-5.218	-.059	-.159	4.138	4.138	1.079	0.463	7.932	0.926
[Cd(HDMAH) Cl_2 (EtOH) H_2O]	-5.642	-2.875	-2.767	4.258	4.258	1.383	0.361	6.553	0.722
[Hg(HDMAH)Cl(OH)EtOH]3EtOH	-5.535	-2.904	-2.631	4.219	4.219	1.315	0.380	6.767	0.760

Table (6). Selected DFT bond length (Å) of HDMAH ligand

Bond	HDMAH	Zn^{2+} complex	Cd^{2+}complex	Hg^{2+}complex
C11-O13	1.281	1.217	1.219	1.225
C15-N14	1.264	1.354	1.271	1.288
C10-S8	1.834	1.815	1.823	1.834
N12 -N14	1.354	1.354	1.357	1.354
C15-H33	1.106	1.112	1.108	1.181
N12-H32	1.016	1.008	1.009	1.009
C15-C16	1.345	1.349	1.347	1.348
C11-N12	1.403	1.365	1.370	1.376
C10-H30	1.148	1.115	1.115	1.136
C10-H31	1.149	1.115	1.115	1.137
M-O	-	1.905,1.905	2.128	2.142
M-N	-	1.941,1.942	2.164	2.184
M-S	-	-	-	2.511
M1-CL	-	2.246	2.471	2.481
M2-O-H	-	1.895	2.141	2.131

Table (7). Selected DFT bond angles (^{0}) of HDMAH ligand and its M(II) complexes.

Bond angle	HDMAH	Zn^{2+} complex	Cd^{2+} complex	Hg^{2+} complex
N(12)-C(11)-C(10)	152.494	115.524,115.32	114.114	115.167
C(16)-C(15)-N(14)	124.318	131.781,124.332	126.606	126.452
C(15)-N(14)-N(12)	121.09	116.536,112.594	114.031	108.183
H(32)-N(12)-C(11)	126.46	121.035,119.906	117.884	118.732
H(32)-N(12)-N(14)	116.238	121.689,121.133	118.676	120.469
N(14)-N(12)-C(11)	117.3	117.178,118.489	122.082	120.79
O(13)-C(11)-N(12)	81.506	119.272,118.622	121.288	124.027
O(13)-C(11)-C(10)	70.988	125.179,125.699	124.577	120.801
H(33)-C(15)-C(16)	120.257	117.404,118.946	117.03	72.283
H(33)-C(15)-N(14)	115.424	110.805,116.695	116.364	71.888
H(30)-C(10)-C(11)	82.116	107.168,107.4	107.678	81.17
H30(17)-C(10)-S(8)	78.854	111.554,111.966	108.73	81.426
H(31)-C(10)-C(11)	82.77	107.871,108.169	107.563	81.003
H(31)-C(10)-S(8)	79.238	111.158,111.24	109.898	81.661

Table (8). ABTS scavenging activity of HDMAH and its metal complexes

Compounds	Absorbance	% inhibition
Control of ABTS	0.510	0
Ascorbic-acid	0.058	88.6
HDMAH	0.138	74.6
Zn L1	0.183	64.1
Cd L1	0.230	54.9
Hg L1	0.281	44.9

Table (9). Erythrocyte Hemolysis (%) of HDMAH and its metal complexes

Compounds	Absorbance	% hemolysis
Absorbance of H_2O (B)	0.820	---
Vit-c	0.035	4.3
HDMAH	0.197	24.0
Zn L1	0.186	22.7
Cd L1	0.189	23.0
Hg L1	0.207	25.2

Conclusion

Preparation, characterization methods, ant hemolysis and $ABTS^+$ scanning activity of the hydrazine (HDMAH) and its corresponding Zn(II), Cd(II) and Hg(II) complexes are described herein. The current metal complexes have an octahedral geometry, with the ligand (HDMAH) functions as a neutral bidentate and coordinating via the nitrogen atom of the azomethine (-C=N-) group and the oxygen of the carbonyl group in the keto form. Theoretical, magnetic, thermal, and spectroscopic evidence all support this. Thermal studies (TGA and DrTGA) as well as the negative values of the energies of Frontier molecular orbitals demonstrate the stability of the compounds (HOMO and LUMO). Also, the compounds were examined for anti hemolysis and $ABTS^+$ scavenging activities and the results obtained indicated……. In other words, the substances mentioned in the title might be useful for medicinal purposes.

References

1. Wilkinson, G.; Gillard, R.D.; McCleverty, J. A. (1987).Comprehensive Coordination Chemistry, vol. **2**, Elsevier, Oxford,
2. Wang, Y., Yang, Z. and Wang, B. Trans. Synthesis, (2005) characterization and anti-oxidative activity of cobalt(II), nickel(II) and iron(II) Schiff base complexes Trans.Met. Chem., **30**, 879-883.
3. Maragerum, D. W.; Owens, G. D.; Sigel, H. (1981) Metal Ions in Biological Systems, vol. **12** , Marcel Dekker Inc., New York, , 75.
4. Chakraborty, J.; Samanta, B.; Pilet, G., Mitra, S. Synthesis, (2006) structure and spectral characterization of a hydrogen-bonded polymeric manganese(III) Schiff base complex, *J. Struct.* Chem., **17**, *585-593.*
5. Shrivastav, A.; Singh, N. K.; Tripathi, P.; George, T.; Dimmock, J. R.; Sharma, R. K., (2006) Copper(II) and manganese(III) complexes of N′-[(2-hydroxy phenyl) carbonothioyl] pyridine-2-carbohydrazide: novel therapeutic agents for cancer. Biochimie., **88**, 1209–1216.
6. Chohan, Z. H.; Pervez, H.; Khan, K. M.; Supuran, C. T. (2005) Organometallic-based antibacterial and antifungal compounds: transition metal complexes of 1,1′- diacetylferrocene-derived thiocarbohydrazone, carbohydrazone, thiosemicarbazone and semicarbazone, *J. Enzyme Inhib. Med. Chem.*, **20**, 81-89.
7. Cristau, H.; Cellier, P. P.; Spindler, J.; Taillefer, M., (2004) Mild Conditions for Copper-Catalyzed N-Arylation of Pyrazoles Eur. *J. Org. Chem.*, **4**, 695-709.
8. De Sousa, G. F.; Mangas, M. B. P.; Francisco, R. H. P.; P. Gambardella; M. T., Rodrigues, A. M. G. D.; Barras, (1999) New Heptacoordinated Organotin(IV) Complexes Derivatives of 2,6-diacetylpyridinebis(2-furanoylhydrazone), H2dapf, and 2,6-diacetylpyridinebis(2-thenoylhydrazone), H_2dapt. Crystal and Molecular Structure of $[Me_2Sn(Hdapt)]Br.H_2O$. *J. Braz. Chem. Soc*., **10**, 222-230.
9. Bacchi, A.; Pelizzi, G.; Jeremić, D.; Sladić, D.; Gruden-Pavlović, M.; Andjelković, K., (2003) Synthesis and structural characterization of copper(II) complexes with the 2¢-[1-(2-pyridinyl)ethylidene]oxalohydrazide ligand, Trans. Met. Chem, **28**, 935-938.
10. Pelizzi, C.; Pelizzi, G.; Predieri, G. (1984) Investigation into aroylhydrazones as chelating agents: V. Synthesis and structural characterization of two seven-coordinate organotin(IV) complexes with 2,6-diacetylpyridine bis(2-aminobenzoylhydrazone). *J. Organometal. Chem*., **263**, 9-20.
11. El-Gammal, O.A., Fouda A.A., Nabih, D.M. (2019) Synthesis, spectral characterization, DFT and in vitro antibacterial activity of Zn(II), Cd(II) and Hg(II) complexes derived from a new thiosemicarbazide; Letters in Applied NanoBioScience, , **8**, 715 – 722.
12. El-Gammal, O.A., Abu El-Reash, G.M., Goama, H.E. Mononuclear Cr(III), Mn (II), and Fe(III) (2019), complexes derived from new ONO symmetrical flexible hydrazone: synthesis, spectral characterization, optical band gap and DFT computational study; Letters in Applied Nano Bioscience, **8**, 743 – 753.

13. Vogel, A. I., A (1994) .text book of quantitative Inorganic Analysis, Longmans, London,
14. Geary, W. J. (1971).The use of conductivity measurements in organic solvents for the characterization of coordination compounds. Coord. Chem. Rev.
15. Modeling and Simulation Solutions for Chemicals and Materials Research. Materials Studio, (2011). Version 7.0, Accelrys software Inc., San Diego, USA,
16. Hammer, B.; Hansen, L. B.; Nørskov, J. K. (1999) Improved adsorption energetics within density-functional theory using revised Perdew-Burke-Ernzerhof functionals. Phys. Rev. B, **59**, 7413-7421.
17. Delley, B.(2000) From molecules to solids with the $DMol^3$ approach. *J. Chem. Phys.*., **113**, 7756-7764.
18. Stylianakis, A. Kolocouris, N. Kolocouris, G. Fytas, G.B. Foscolos, E. Padalko, J. Neyts, D. Clerq, E. Spiro [pyrrolidine-2, 2′-adamantanes]: (2003) synthesis, anti-influenza virus activity and conformational properties. Bioorg, Med. Chem. Lett., **13**, 1699 – 1703.
19. Wolfe, A.; Shimer, G.H (1987); Meehan, T. Polycyclic aromatic hydrocarbons physically intercalate into duplex regions of denatured DNA. Biochem. **26**, 6392–6396.
20. El-Gammal, O. A.; Abu El-Reash , G.M.; Ahmed, S. F. (2012) Structural, spectral, thermal and biological studies on 2-oxo-N′-((4-oxo-4H-chromen-3-yl)methylene)-2-(phenylamino)acetohydrazide (H2L) and its metal complexes. *J. Mol. Struct.*,1007, 1-10.
21. El-Gammal, O. A.; Abu El-Reash, G.M.; Ghazy, S.E.; Radwan, A.H.; (2012) Synthesis, characterization, molecular modeling and antioxidant activity of (1E,5E)-1,5-bis(1-(pyridin-2-yl)ethylidene)carbonohydrazide (H2APC) and its zinc(II), cadmium(II) and mercury(II) complexes. *J. Mol. Struct*., **1020**, 6-15.
22. El-Asmy, A.A.; El-Gammal, O.A.; Radwan, H.A. Ligational, (2010),analytical and biological applications on oxalyl bis(3,4-dihydroxybenzylidene) hydrazone. *J. Spectrochim Acta*, Part A; **77**, 297–303.
23. El- Gammal, O.A. ; El-Shazly, R.M. ; El-Morsy, F.E. ; El-Asmy, A.A(2011),. Synthesis, characterization, molecular modeling and antibacterial activity of N1/, N2/-bis[1-(pyridin-2-yl)ethylidene]oxalohydrazide and its metal complexes. *J. Mol. Struct.* **998**, 20-29.
24. El-Gammal,O.A.; Rakha, T.H.; Metwally, H.M. ; Abu El- Reash, G.M.; (2014)Synthesis, characterization, DFT and biological studies of isatin picolinohydrazone and its Zn(II), Cd(II) and Hg(II) complexes. Spectrochimica Acta Part A:, **127**, 144–156.
25. El-Gammal, O.A (2015). Mononuclear and binuclear complexes derived from hydrazone Schiff base NON donor ligand: Synthesis, structure, theoretical and biological studies"Inorganica Chimica Acta, ,**435**, 73–81.
26. Al-Adilee, Kh. ; Kyhoiesh, H.A.K. (2017),Preparation and identification of some metal complexes with new heterocyclic azo dye ligand 2-[2-- (1-Hydroxy -4- Chlorophenyl) azo]-imidazole and their spectral and thermal studies, *J. Mol. Struct.* **1137**, 160-178.
27. Okagu, O. D.; Ugwu, K. C.; Ibeji, C. U.; Ekennia, A. C.; Okpareke, O. C.; Ezeorah, Ch. J.; Anarado, Ch. J.O.; Babahan, I.; Coban, B. ; Yıldız, U.; Comert, F.; Ujam, O. T. (2019) ,Synthesis and characterization of Cu(II), Co(II) and Ni(II) complexes of a benzohydrazone derivative: Spectroscopic, DFT, antipathogenic and DNA binding studies. *J. of Mol. Struct.* **1183**, 107-117.
28. El-Gammal, O. A.; Abu El-Reash , G.M.; Ahmed, S. F. (2015) Synthesis, biological and comparative DFT studies on Ni(II) complexes of NO and NOS donor ligands Spectrochimica Acta Part A: Molecular and Biomolecular Spectroscopy,**135**,690–703.
29. Castiǵeiras A., Gómez M. C., Hiller W., (1992) "Structure oftetrakis(N,N dimethylbenzenecarbothioamide-*S*)cadmium(II)diperchlorate

monohydrate", Acta Crystallographica Section *C*, **48**, 2215-2218.
30. Sawada, T.; Fukumaru, K.; Sakurai, H. L-band ESR spectra of copper(II) (1995),complexes with CuN4 configurations. Biochem Biophys Res Commun. **216**, 154-161.
31. Shimizu, I.; Morimoto, Y.; Faltermeier, D.; Kerscher, M.; Paria, S.; Abe, T.; Sugimoto, H.; Fujieda, N.; Asano, K.; Suzuki, T.; Comba, P.; Itoh, S. (2017) Tetrahedral Copper(II) Complexes with a Labile Coordination Site Supported by a Tris-tetramethylguanidinato Ligand. Inorg. Chem., **56**, 9634-9645.
32. Hatakeyama, T.; Quinn, F. X. (1994)Thermal Analysis Fundamentals and Applications to Polymer Science, 2nd ed., John Wiley and Sons, Chichester,.
33. Maravalli, P. B.; Goudar, T. R. (1999),Thermal and spectral studies of 3-N-methyl-morpholino-4-amino-5-mercapto-1,2,4-triazole and 3-N-methyl-piperidino-4- amino-5-mercapto-1,2,4-triazole complexes of cobalt(II), nickel(II) and copper(II) Thermochim. Acta **325**, 35-41.
34. El-Gammal, O. A. (2010),Synthesis, Characterization and Antimicrobial Activity of 2-(2-ethylcarbamothioyl)hydrazinyl)-2-oxo-N-phenylacetamide copper complexes. Spectrochim. Acta Part A. **75**, 533-542.
35. El-Gammal, O. A.; Bekheit, M. M.; El-Brashy, S. A. (2015),Synthesis, characterization and in-vitro antimicrobial studies of Co (II), Ni (II) and Cu (II) complexes derived from macrocyclic compartmental Ligand. Spectrochimica Acta Part A **137**, 207-219.
36. Fukui, K.; Yonezawa, K.; Nagata, C.; Shingu, H. (1997) Molecular orbital theory of orientation in aromatic, heteroaromatic, and other conjugated molecules, in: Frontier Orbitals And Reaction Paths: Selected Papers of Kenichi Fukui, World Scientific,; pp. 33-42.
37. Luque, F. J.; López, J. M.; Orozco, M. Perspective on (2000) "Electrostatic interactions of a solute with a continuum. A direct utilization of ab initio molecular potentials for the prevision of solvent effects". Theor. Chem. Acc., **103**, 343-345.
38. Politzer, P.; Laurence, P. R.; Jayasuriya, K. (1985) Molecular electrostatic potentials: an effective tool for the elucidation of biochemical phenomena. Environ Health Perspect., , **61**, 191-202.
39. O.A. El-Gammal, F.Sh. Mohamed, G.N. Rezk, A.A. El-Bindary, (2021) *J. Mol. Liq*. 326 115223.
40. O.A. El-Gammal. (2010). "Synthesis, Characterization and Antimicrobial Activity of 2-(2-ethylcarbamothioyl)hydrazinyl) -2-oxo-N-phenylacetamide copper complexes" Spectrochim Acta Part A., 75, 533
41. O.A. El-Gammal,. (2015) "Mononuclear and binuclear complexes derived from hydrazone Schiff base NON donor ligand: Synthesis, structure, theoretical and biological studies" Inorg. Chim. Acta **435** 73–81.
42. O.A. El-Gammal, G.M. Abu El-Reash, S.E. Ghazy, A.H. Radwan" (2012). Synthesis, characterization, molecular modeling and antioxidant activity of (1E, 5E)-1,5- bis(-pyridin-2-yl)ethylidene) carbohydrazide (H2APC) and its zinc(II) , cadmium(II) and mercury (II) complexes" *J.Mol. Struct.***1020**, 6-15
43. O. A. El-Gammal, G. M. Abu El-Reash, and M. M. El-Gamil" (2013)." Novel Mercury (II), Cadmium(II) and Binuclear Zinc (II) complexes of N1-ethyl-N2-(pyridine-2-yl) hydrazine-1, 2-bis (carbothioamide): structural, spectral, pH-metric and biological studies" Spectrochimica Acta Part A: **59** -70